

# A Stochastic Theory of Phase Transitions in Human Hand Movement

G. Schöner<sup>1</sup>, H. Haken<sup>1</sup>, and J. A. S. Kelso<sup>2</sup>

<sup>1</sup> 1. Institut für theoretische Physik, Universität Stuttgart, Pfaffenwaldring 57/4, D-7000 Stuttgart 80, Federal Republic of Germany

<sup>2</sup> Haskins Laboratories, New Haven, Connecticut, USA  
Department of Psychology, University of Connecticut, Storrs, Connecticut, USA

**Abstract.** The order parameter equation for the relative phase of correlated hand movements, derived in a previous paper by Haken et al. (1985), is extended to a time-dependent stochastic differential equation. Its solutions are determined close to stationary points and for the transition region. Remarkably good agreement between this theory and recent experiments done by Kelso and Scholz (1985) is found, and new predictions are offered.

## 1 Introduction

In recent experiments by Kelso (1981, 1984) a remarkable transition between two different modes of human hand movement was found, namely between an antiphase motion of relative phase  $\phi = \pi$  involving nonhomologous muscle groups, and an in-phase motion with relative phase  $\phi = 0$  that involved homologous muscles. These experimental results were successfully modeled by Haken et al. (1985). However, though the latter paper already suggested that fluctuations were important for the occurrence of this transition, no explicit attempt at a quantitative treatment of the role of fluctuations was made at that time. In this paper we develop a stochastic model of the phase transition that turns out to be in good agreement with recent experiments (Kelso and Scholz 1985) in which fluctuations were explicitly measured.

The current work attests to the usefulness of synergetic concepts in modeling complex systems that are governed by order parameter equations (Haken 1975, 1983). Such a synergetic treatment allows one to interpret observed changes in behavioral pattern between the hands as a nonequilibrium phase-transition, a phenomenon nowadays found in a variety of physical, chemical, and biological systems (see e.g., Haken 1983). Thus, a rather different account of "switching"

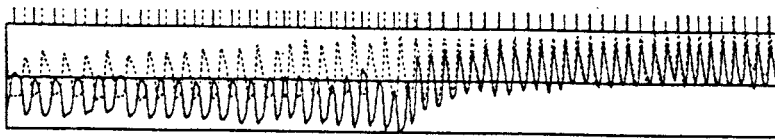
among spatiotemporal movement patterns is offered by synergetics, one that contrasts sharply with theoretical accounts that posit distinct motor programs (cf. Schmidt 1982) for each new pattern (e.g., the locomotor gaits). In synergetics, new (or different) modal patterns arise as a result of instabilities that occur as a system is scaled away from its "preferred" equilibrium state. Though pattern generation *emerges* as a consequence, it is not necessary to introduce a priori special mechanisms, such as motor programs to explain such pattern formation. Importantly, the identity between these abrupt shifts in behavioral pattern with a nonequilibrium phase transition leads, as we shall see, to new and testable predictions that have not come to light in more standard accounts.

The present paper is organized as follows: First, we shall describe briefly the experimental set-up and the main experimental results to be treated in-depth here. These focus principally on new experiments that deal with the stochastic aspects of the transition. In Sect. 3 we shall present the basic model, and then, in Sect. 4 deal explicitly with theoretical stochastic properties. There we shall treat both the transition region itself as well as the surrounding stationary states in relative phase. This section will be concluded by a calculation of the first passage time.

## 2 Experimental Stochastic Properties

In the original experiments (Kelso 1981, 1984), subjects were initially instructed to cycle their fingers or hands at a preferred frequency using an out-of-phase motion. The driving frequency,  $F$ , measured in Hz, was then increased in a continuous fashion. At a critical frequency, a transition from one state with relative phase  $\phi = \pm \pi$  (referred to as the antisymmetric mode) to another state with relative phase  $\phi = 0$  (referred to as the symmetric mode) occurred. Below the transition point the system was bistable, i.e., two stable phase (or

## A. TIME SERIES



## B. POINT ESTIMATE OF RELATIVE PHASE

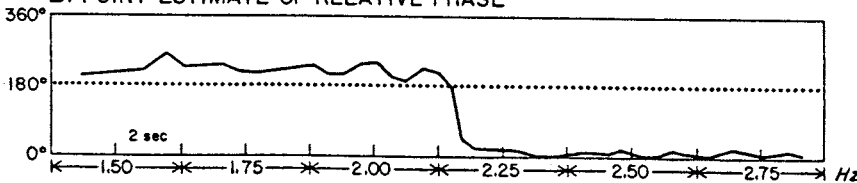


Fig. 1. A Time series showing position over time of left (*dashed line*) and right (*solid line*) index fingers as the control parameter,  $F$ , is systematically scaled. B The corresponding point estimate of relative phase, i.e., the phase of one finger's oscillatory peak relative to the other (see text for details)

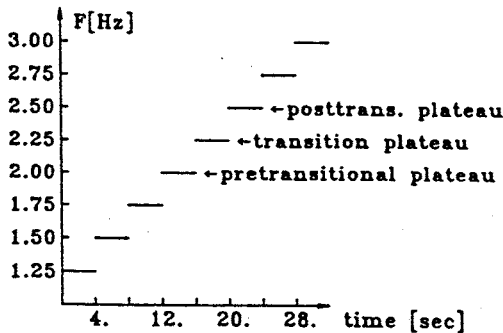


Fig. 2. Schematic drawing of the temporal evolution of the experimental control parameter frequency. In this case, which refers to Fig. 1, the transition occurred at 2.25 Hz

“attractor”) states between the hands could be realized. Beyond the critical frequency only the symmetric mode persisted, at least within the range of driving frequencies examined.

In more recent experiments (a preliminary account of which is given in Kelso and Scholz 1985), that were designed to explore in more detail the stochastic properties of the transition, subjects oscillated the index fingers bilaterally in the transverse plane (i.e., abduction-adduction). Continuous finger displacement in two planes of movement was measured using a modified Selspot camera system. The electromyographic (EMG) activity of the right and left first dorsal interosseus (FDI) and first volar interosseus (FVI) muscles were obtained using platinum fine wire electrodes (see Kelso and Scholz, Fig. 4). In the experiment of prime interest here, the control parameter,  $F$ , was systematically increased in 0.25 Hz steps at 4-s intervals according to a metronome pacing stimulus. Data from trials in this experiment could therefore be time-averaged. Figure 1 presents measurements which exhibit the phase transition nature of the phenomenon, and Fig. 2 illustrates how  $F$  was increased in a step-wise manner. Several time-scales can be identified in the experiment.

The length of the frequency plateau (4 s) shown in Fig. 2 constitutes the experimental time scale for change of control parameter  $\tau_p = 4$  s. The measured mean absolute value of relative phase  $\langle |\phi| \rangle$  and its standard deviation (SD) are depicted in Fig. 3.<sup>1</sup> Note that  $\langle |\phi| \rangle$  and SD in the symmetric mode are roughly constant through all parameter values. The constants are  $\langle |\phi| \rangle \approx 8$  deg and  $SD \approx 4.5$  deg.

In the antisymmetric mode below the transition the mean absolute phase decreases, while SD increases as the transition is approached. In the transition region the SD reaches a maximum, while  $\langle |\phi| \rangle \approx 85$  deg, a value that almost corresponds to an equidistribution (for which  $\langle |\phi| \rangle = 90$  deg). Above the transition the data of antisymmetrically and symmetrically prepared experiments coincide. Outside the transition region the behavior is stationary on the observed time scale of  $\tau_p = 4$  s. This was checked explicitly in the Kelso and Scholz data by calculating mean and variance for several 0.5 s time windows on these plateaus. On the transition plateau transients occur. These can be seen in the time plots of relative phase (Fig. 1) and were checked with the statistical data as mentioned above. The typical time it takes the system to reach its new state, the so-called transient time,  $\tau_{trans}$ , has not yet been measured systematically. However, from the present data a preliminary estimate is  $\tau_{trans} = 1$  to 2 s (cf. Fig. 1).

Another relevant time scale is that of the local relaxation times  $\tau_{rel}$ . These are the times it typically takes the system to reach one of the stationary states [i.e., the symmetric ( $\phi_{stat} = 0$ ) or the antisymmetric mode ( $\phi_{stat} = \pm \pi$ )] from a somewhat perturbed state ( $0 < |\phi - \phi_{stat}| \leq 1$ ). These local relaxation times have

1 Note that these data are based on the *point* estimate of relative phase (cf. Fig. 1), not the continuous estimate as erroneously indicated in Kelso and Scholz (1985, Fig. 6). When time averaged, however, both estimates yield a near-identical pattern of results. The data based on a continuous estimate of relative phase are available from the third author

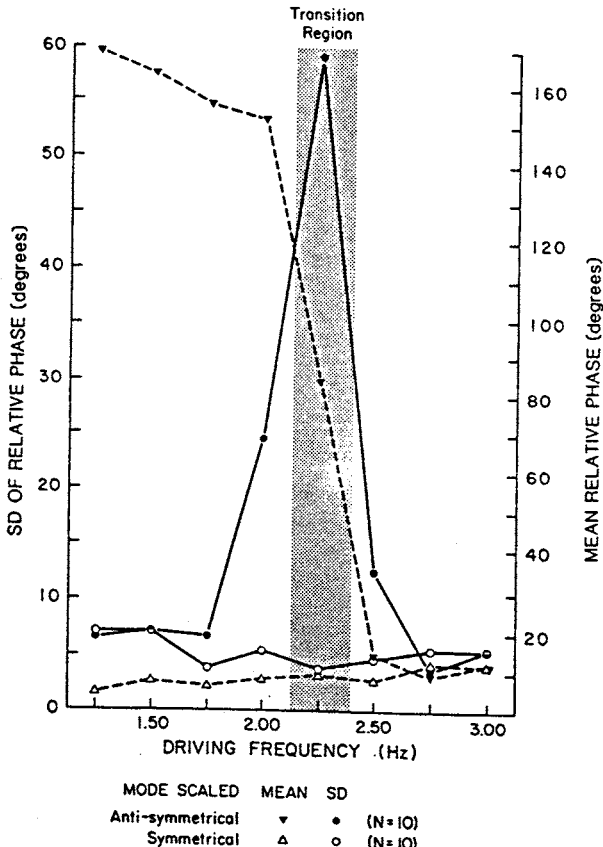


Fig. 3. The mean phase modulus  $\langle|\phi|\rangle$  ( $\nabla$  AMS,  $\Delta$  SMS) and its SD =  $\{\langle\phi^2\rangle - \langle|\phi|\rangle^2\}^{1/2}$  ( $\bullet$  AMS,  $\circ$  SMS) were determined in the stationary limit on each frequency plateau (i.e. for the last 3 s at each frequency). Each point on the graph represents an average from 10 runs of the experiment. AMS=antisymmetric mode scaled, SMS=symmetric mode scaled (from Kelso and Scholz 1985)

not yet been measured systematically either, but an estimate can be made based on the time the subjects need to adapt to a change in driving frequency. An upper bound for this time is that of one cycle. Hence  $\tau_{rel} \leq 0.33$  s to 0.8 s at driving frequencies between 1.25 Hz and 3.0 Hz. We choose  $\tau_{rel} = 0.25$  s as an estimate. This seems to be a reasonable assumption in light of the fact that reaction times in other skills (like car driving) are of the same order of magnitude (cf. e.g. Kelso et al. 1979). In the theoretical considerations of Sect. 4 all calculations were repeated also for parameters based on an estimate of  $\tau_{rel} = 0.5$  s and no qualitative difference was observed.

### 3 Model

In an attempt to model the stochastic properties of the experimental system described above we can profit from the model developed previously by Haken et al. (1985). In their work the relative phase  $\phi$  was identified

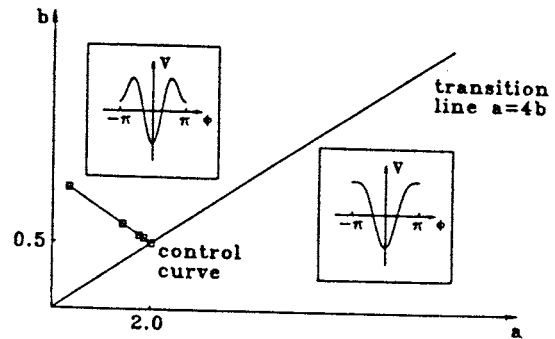


Fig. 4. A phase portrait of  $V$  in the parameter plane  $(a, b)$ . The regime, where  $\phi = 0$  is the only minimum is separated from a regime with two minima at  $\phi = \pm\pi$  and  $\phi = 0$  resp. by the transition line. We restrict ourselves to  $a > 0$ ,  $b > 0$ , because the transition line lies completely in this domain. The insets illustrate the form of the potential in the two regimes. The control curve, on which the experimental system moves through the transition has been included. This was determined from experimental data and local models (cf. Sect. 4.3)

as an order parameter in the sense of synergetics and a relaxational equation of motion for  $\phi$  was determined from the attractor layout:

$$\dot{\phi} = -\frac{\partial V}{\partial \phi}, \quad (3.1)$$

where

$$V(\phi) = -a \cos \phi - b \cos 2\phi = V(\phi + 2\pi) \quad (3.2)$$

is a periodic potential and  $a$  and  $b$  are model parameters. We can restrict  $\phi$  to  $[-\pi, \pi] \bmod 2\pi$  with the identification  $\pi = -\pi$ . In Fig. 4 the attractor layout is illustrated for the potential (3.2) (cf. Haken et al. 1985). Minima of the potential correspond to stable, stationary states  $\phi_{stat}$ , that can be prepared experimentally (i.e.  $\dot{\phi}_{stat} = 0$  and  $\phi_{stat} = \pm\pi$ ).

In their work Haken et al. go on to derive the order parameter dynamics from a model of two nonlinearly coupled, nonlinear oscillators. In this paper we restrict ourselves to an analysis of the system's fluctuational character at the level of the order parameter,  $\phi$ .

To account for the fluctuations present in the experimental data (cf. Fig. 1) we add to the equation of motion (3.1) a stochastic force in an ad hoc fashion:

$$\dot{\phi} = -\frac{\partial V}{\partial \phi} + \sqrt{Q} \xi_t, \quad (3.3)$$

where  $\xi_t$  is a Gaussian white noise process with

$$\langle \xi_t \rangle = 0; \quad \langle \xi_t \xi_{t'} \rangle = \delta(t - t') \quad (3.3a)$$

and  $Q > 0$  is the noise strength (a third model parameter). This process has to be taken modulo  $2\pi$  to make  $\phi_t$  a stochastic process on the circle of radius one  $[-\pi, \pi] \bmod 2\pi$ . The rationale for using this particular

choice of stochastic force is the assumption that the degrees of freedom acting as noise on the system live on a time scale that is much faster than the time scale of  $\phi$ . This approximation is usually good near bifurcations due to the slowing down of the order parameter (cf. Sect. 4 for details). In other words we do not expect the stochastic properties to depend qualitatively on the details of the dynamics of  $\xi_t$  near the transition. [For more information on the nature of stochastic forces see e.g. Haken (1983, Chap. 6).]

The stochastic process defined by the so called Langevin Eq. (3.3) is a Markov process that is completely characterized by the transition probability  $P(\phi, t|\phi', t')$  and the one-time probability distribution  $P(\phi, t)$ . (All distributions in this paper are distribution densities really.) These functions obey a Fokker-Planck equation that is completely equivalent to the Langevin Eq. (3.3) and reads:

$$\dot{P}(\phi, t) = \frac{\partial}{\partial \phi} \{V(\phi)P(\phi, t)\} + \frac{Q}{2} \frac{\partial^2}{\partial \phi^2} P(\phi, t). \quad (3.4)$$

[For an introduction to these concepts consult e.g. Haken (1983, Chaps. 4 and 6), or Gardiner (1983).]

## 4 Theoretical Stochastic Properties

### 4.1 Times Scales

In the experiment described in Sect. 2 above, there are basically three theoretically relevant time scales:

(a) The scale of local relaxation times  $\tau_{rel}$ . Such relaxation times measure how long a transient to one of the stationary modes from a mode "nearby" typically takes. In this context the stationary modes are just  $\phi_{stat} = 0$  and  $\phi_{stat} = \pm \pi$  and a mode "nearby" means a relative phase close to 0 or  $\pm \pi$  resp. A more precise definition of  $\tau_{rel}$  will be given below (Sect. 4.2) in terms of correlation times. Our estimate for  $\tau_{rel}$  outside the transition region was  $\tau_{rel} = 0.25$  s in either mode (cf. Sect. 2).

(b) The observed time scale on which averages are performed. This includes times from  $\tau_{rel}$  up to the time scale of change of parameter  $\tau_p$ , which was 4 s in Kelso and Scholz (1985).

(c) The time scale of equilibration  $\tau_{equ}$ . This is a somewhat more abstract concept in the present experimental context. Let us explain it first in terms of the stochastic model (2.3). In this model equilibration means that the stationary distribution of phase, i.e. the solution of  $\dot{P}(\phi, t) = 0$ , is realized. Approach to equilibrium means that an initial distribution evolves in time such that it finally becomes the stationary distribution. The equilibration time is the time this typically takes. (See also Sect. 4.5 for a quantitative measure of  $\tau_{equ}$  in the bistable potential.) Due to the presence of a

stochastic force, that can time and again push the system to any point in  $[-\pi, \pi]$ , the stationary distribution is always a distribution that feels all of the potential, i.e. with finite, though possibly very small probability, any subinterval can be occupied. In the bistable potential below the transition, for example, the stationary distribution has peaks at both stationary states (although that at  $\phi = 0$  is larger).

How do these time scales impact on the interpretation of the phase transition? Below the transition the equilibrium state in the experiment would be one in which the system may occasionally switch from one stationary state to the other. In effect, the system can spend a certain amount of time in each stationary state, that amount being proportional to the height of the corresponding peak of the stationary distribution. Effects of the initial preparation would not be felt anymore. No such switching between the two modes can be observed below the transition, however. We infer that  $\tau_{equ}$  is much larger than observed times:  $\tau_{equ} \gg \tau_p$ , so that equilibration does not happen in the experiment. At the transition we do indeed observe one switching and infer that  $\tau_{equ}$  has sufficiently decreased. A switching back to the now unstable antisymmetric mode, however, is so unlikely, that it cannot be seen in the observed time.

In summary we expect in the present experiment the following time scales relation to hold sufficiently far below the transition:

$$\tau_{rel} \ll \tau_p \ll \tau_{equ}. \quad (4.1)$$

At the transition  $\tau_{equ}$  comes down to the observed time scale  $\tau_p$ , while one of the relaxation times (that with respect to the stationary state  $\phi_{stat} = \pm \pi$ ) is expected to increase to the level of  $\tau_p$ . These two points will be discussed in much more detail below.

What are the implications of this analysis for the theory? First, this relation shows that the discussion of the qualitative behavior of the model in terms of potential minima (cf. Sect. 3) is consistent. Second, in the present study of the stochastic properties of the model, the arguments above require us to differentiate between two regimes: (a) The pre- (and post-) transition regimes in which the system obeys the time scales relation (4.1). Thus we model it by local models of the state, in which the system is prepared. In these local models, which possess only one stationary state, we perform the stationary limit time to infinity (cf. Sects. 4.2 and 4.3); and (b) The transition regime itself, in which we expect transients to occur. Thus we study the temporal evolution of the distribution of  $\phi$  as governed by the full dynamics of (3.4). As initial distribution we shall use the stationary distribution of the local model of the antisymmetric mode corresponding to the last pretransitional parameter plateau (cf. Sect. 4.4).

## 4.2 Local Model of Symmetric Mode

We expand the equation of motion of  $\phi$  about the deterministic stationary solution  $\phi_{\text{stat}} = 0$  and obtain in first order:

$$\dot{\phi} = -(4b + a)\phi + \sqrt{Q}\xi, \quad (4.2)$$

which corresponds to overdamped motion in a quadratic potential illustrated in the inset of Fig. 5. We can calculate the stationary distribution of  $\phi$  exactly from the Fokker-Planck equation corresponding to this linear Langevin equation. From the stationary distribution we obtain the stationary moments as:

$$\langle |\phi| \rangle_{\text{stat}} = \int_{-\infty}^{\infty} d\phi |\phi| P_{\text{stat}}(\phi) = \frac{1 - \exp(-\pi^2 d^2)}{\sqrt{\pi} d \operatorname{erf}\{\pi d\}} \quad (4.3)$$

and

$$\sigma_{\text{stat}} = \langle \phi^2 \rangle_{\text{stat}} - \langle |\phi| \rangle_{\text{stat}}^2 = \frac{1}{2d^2} - \frac{\sqrt{\pi} e^{-\pi^2 d^2}}{d \operatorname{erf}\{\pi d\}} - \langle |\phi| \rangle_{\text{stat}}^2. \quad (4.4)$$

In these expressions the dependence on the parameters  $a$ ,  $b$ , and  $Q$  condenses into a dependence on

$$d = \sqrt{\frac{4b + a}{Q}}. \quad (4.5)$$

In Fig. 5 the mean absolute phase  $\langle |\phi| \rangle_{\text{stat}}$  and the corresponding standard deviation  $\text{SD} = \sqrt{\sigma_{\text{stat}}}$  are plotted as a function of  $d$ . The limit  $d \rightarrow 0$  corresponds to an infinite noise level, where the stationary distribution is an equidistribution. The limit  $d \rightarrow \infty$  corresponds to no noise. The mean is then the deterministic value  $|\phi| = 0$  and SD is zero. The data of Fig. 3 show that  $\langle |\phi| \rangle_{\text{stat}}$  and SD are in experiment roughly constant for all driving frequencies. From the experimental

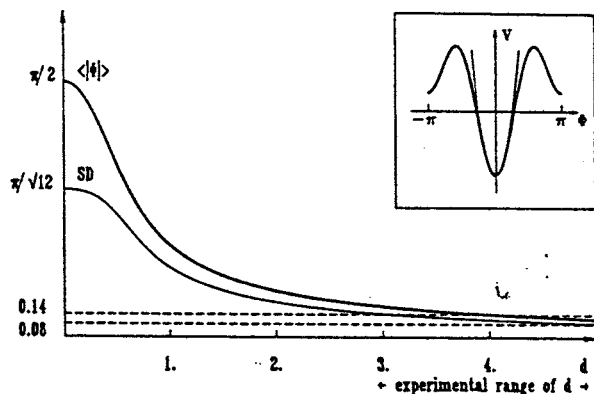


Fig. 5. The mean phase modulus and its SD as calculated from the local model of the symmetric mode ( $\phi_{\text{stat}} = 0$ ), as a function of  $d = \{(a + 4b)/Q\}^{1/2}$ . Two lines indicate the experimental values for mean ( $\approx 0.14$ ) and SD ( $\approx 0.08$ ), so that experimentally realistic values for  $d$  can be read off. The inset shows a sketch of the potential (*fat*) and the local model (*thin*) at  $a = b = 1$ . Hz

values for mean and SD we can determine via the functions of Fig. 5 the values of the parameter  $d$  corresponding to the experimental situation. Using a mean of  $\langle |\phi| \rangle_{\text{stat}} \approx 8$  deg we find  $d$  in the range 3. to 5. The experimental value of  $\text{SD} \approx 4.5$  deg yields approximately the same range for  $d$  (this is a check on the range of  $d$  through a second measured quantity). Thus we can use as an estimate:  $d \approx 4$ . Note that this, as well as all subsequent estimates for model parameters are meant to determine the adequate order of magnitude only.

The local relaxation time can conveniently be discussed in terms of this local model. A deterministic definition of local relaxation time is the following:  $\tau_{\text{rel}}$  is the typical time in which a small deviation from the stationary solution  $\phi_{\text{stat}} = 0$  decays<sup>2</sup>. A solution of the deterministic linear equation of motion

$$\phi(t) = \phi(0) \exp[-(4b + a)t] \quad (4.6)$$

immediately shows that

$$\tau_{\text{rel}} = \frac{1}{4b + a} = \frac{1}{d^2 Q}. \quad (4.7)$$

A more general definition of  $\tau_{\text{rel}}$ , that takes the stochasticity of  $\phi_t$  into account, makes use of the stationary correlation function:

$$\langle \phi_t \phi_0 \rangle_{\text{stat}} = \lim_{t' \rightarrow \infty} \langle \phi_{t+t'} \phi_{t'} \rangle \quad (4.8)$$

( $\lim_{t' \rightarrow \infty}$  means: for  $t'$  large enough for the average not to depend on  $t'$  any more). One can define  $\tau_{\text{rel}}$  then through<sup>2</sup>

$$\tau_{\text{rel}} = \frac{1}{\langle \phi^2 \rangle_{\text{stat}}} \int_0^{\infty} dt \langle \phi_t \phi_0 \rangle_{\text{stat}}. \quad (4.9)$$

Unfortunately it is impossible even in this linear model to calculate the stationary correlation function (4.8) exactly due to the periodic boundary conditions:  $\phi \in [-\pi, \pi]$  with  $\pi \equiv -\pi$ . In an approximation we extend the range of  $\phi$  to  $(-\infty, \infty)$ . This is a good approximation everywhere, because  $\phi_{\text{stat}} = 0$  is a stable stationary solution, so that  $\phi_t$  will depart from the vicinity of 0 only with negligible probability. In that approximation  $\phi_t$  is an Ornstein-Uhlenbeck process with

$$\langle \phi_t \phi_0 \rangle_{\text{stat}} = \frac{Q}{2(4b + a)} e^{-t/\tau_{\text{rel}}}, \quad (4.10)$$

where  $\tau_{\text{rel}}$  is given by (4.7). A convenient way to determine  $\tau_{\text{rel}}$  is to read it off the Fourier-transform of the stationary correlation function:

$$C(\omega) = \int_{-\infty}^{\infty} dt e^{i\omega t} \langle \phi_t \phi_0 \rangle_{\text{stat}} = \frac{Q}{\omega^2 + \tau_{\text{rel}}^{-2}}. \quad (4.11)$$

<sup>2</sup> These definitions can be used to devise a measurement procedure

Obviously  $\tau_{rel}^{-1}$  is just the line width of this Lorentzian spectrum.

If we use the experimental estimate for  $\tau_{rel}$  of 0.25 s (cf. Sect. 3) and the value for  $d \simeq 4$ , determined above, we can give an estimate for the noise level in the system:  $Q \simeq 0.25$  Hz.

### 4.3 Local Model of the Antisymmetric Mode

We are now concerned with the stationary state  $\phi_{stat} = \pm \pi$ , which is stable only below the transition, i.e. for  $a < 4b$ . To write down a linear equation of motion for small deviations from  $\phi_{stat} = \pm \pi$  it is convenient to introduce a new variable  $\varepsilon \in [-\pi, \pi]$ :

$$\varepsilon = \begin{cases} \phi - \pi & \text{for } 0 < \phi \leq \pi \\ \phi + \pi & \text{for } -\pi < \phi \leq 0. \end{cases} \quad (4.12)$$

We can now expand the equation of motion about  $\phi_{stat} = \pm \pi$  by expanding in  $\varepsilon$  to first order:

$$\dot{\varepsilon} = -(4b - a)\varepsilon + \sqrt{Q} \xi_t. \quad (4.13)$$

Figure 6 illustrates the corresponding local potential. Mathematically this model is completely equivalent to that of Sect. 4.2 with the mere substitutions  $\phi \rightarrow \varepsilon$  and  $(4b + a) \rightarrow (4b - a)$ . Still we exhibit the results explicitly, because their interpretation is quite different and important for understanding the experiment. The stationary distribution can be determined as before and reads:

$$P_{stat}(\varepsilon) = \frac{f}{\pi \operatorname{erf}\{\pi f\}} e^{-f^2 \varepsilon^2}, \quad (4.14)$$

where

$$f = \sqrt{\frac{4b - a}{Q}}. \quad (4.14a)$$

Note that  $f$  is positive below the transition and approaches zero from above at the transition. The mean modulus is then:

$$\langle |\phi| \rangle_{stat} = \pi - \langle |\varepsilon| \rangle_{stat} = \pi - \frac{1 - \exp(-\pi^2 f^2)}{\sqrt{\pi} f \operatorname{erf}\{\pi f\}} \quad (4.15)$$

and its variance is

$$\begin{aligned} \sigma_{stat} &= \langle \phi^2 \rangle_{stat} - \langle |\phi| \rangle_{stat}^2 = \langle \varepsilon^2 \rangle_{stat} - \langle |\varepsilon| \rangle_{stat}^2 \\ &= \frac{1}{2f^2} - \frac{\sqrt{\pi} \exp(-\pi^2 f^2)}{f \operatorname{erf}\{\pi f\}} - \langle |\varepsilon| \rangle_{stat}^2. \end{aligned} \quad (4.16)$$

We have plotted  $\langle |\phi| \rangle_{stat}$  and  $SD = (\sigma_{stat})^{1/2}$  as a function of  $f$  in Fig. 7. We can now use the experimental data for  $\langle |\phi| \rangle$  to determine from the result of the local model the values of the parameter  $f$  corresponding to each pretransitional parameter plateau.

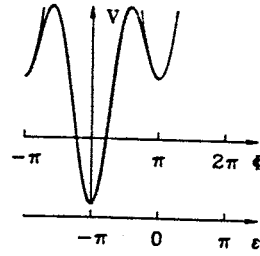


Fig. 6. The potential  $\langle V(\phi) \rangle$  for  $a = b = 1.0$  Hz. The thin curve depicts the corresponding local potential. The variable  $\varepsilon$  is in effect centered at  $\phi = \pi$

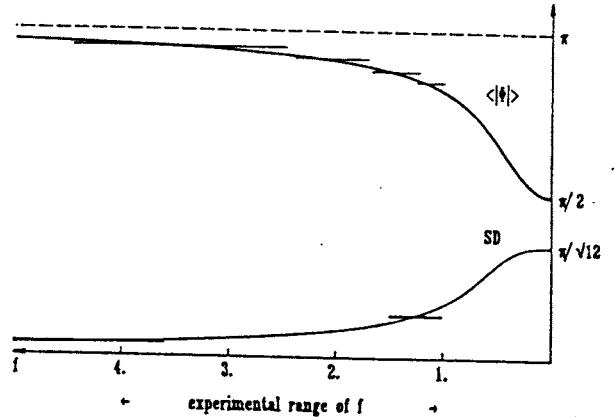


Fig. 7. The mean absolute phase and its SD for the local model of the antisymmetric mode as a function of  $f = [(4b - a)/Q]^{1/2}$ . Approach of the transition corresponds to  $f \rightarrow 0$ . The  $f$ -axis was oriented to the left to illustrate this. The curves have been used to determine from experimental values of mean and SD the corresponding values of  $f$ . The range of such values is indicated

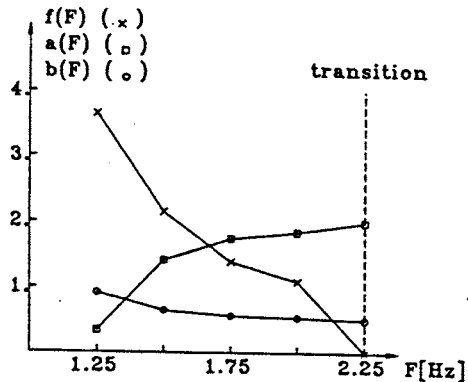


Fig. 8. The model parameters  $f$ ,  $a$  and  $b$  as a function of the experimental control parameter frequency  $F$  as determined from the data on mean and SD and an estimate of relaxation time

This has been done with the help of Fig. 7. The resulting function  $f(F)$ , where  $F$  is the experimental driving frequency, is shown in Fig. 8. The range of  $f$  extends from 4. to 1., with the plateau immediately preceding the transition corresponding  $f_{pre} = 1.1$ . The data for SD give us the opportunity to check these estimates. We observe that these experimental values

are consistent with the above range of  $f$ , with the last pretransitional plateau consistently corresponding to  $f_{\text{pre}} = 1.2$ .

Analogously to the considerations in Sect. 4.2 we can calculate the deterministic local relaxation time as

$$\tau_{\text{rel}} = \frac{1}{4b-a} = \frac{1}{f^2 Q}. \quad (4.17)$$

Although completely analogous to our previous result for the symmetric mode, this expression behaves quite differently near the transition. Due to the fact that  $d$  is roughly constant for all frequencies (as exhibited by constant  $\langle |\phi| \rangle$  and SD of the symmetric mode) and on the assumption that the noise level does not change drastically through the transition<sup>3</sup>, the local relaxation time of the symmetric mode hardly changes at all as frequency is scaled. Quite to the contrary, the relaxation time of the antisymmetric mode diverges as  $f$  approaches the transition. While the divergence is an artefact of the linear approximation, a strong increase of the local relaxation time is predicted also by nonlinear theories. In this experimental setup an upper bound on  $\tau_{\text{rel}}$  will be  $\tau_p$ . This increase in relaxation time of the mode that turns unstable at the transition, is called critical slowing down and is characteristic of this kind of bifurcation phenomenon. Detailed experiments, that determine the local relaxation time of the antisymmetric mode as the system is scaled through the transition are presently under way. They can serve as an additional check on the phase transition character of the present phenomenon.

As discussed already in Sect. 4.2 a more precise definition of  $\tau_{\text{rel}}$  can be phrased in terms of the stationary correlation function. We calculate this correlation function for the present local model again in the approximation that  $\varepsilon$  ranges from  $-\infty$  to  $\infty$ . The result is:

$$\langle \varepsilon_t \varepsilon_0 \rangle_{\text{stat}} = \frac{Q}{2(4b-a)} e^{-t/\tau_{\text{rel}}}, \quad (4.18)$$

where  $\tau_{\text{rel}}$  is identical to that of (4.17). Note that this approximation fails very close to the transition, where the local potential becomes flat, so that the system departs from  $\varepsilon=0$  with increasing probability. The actual experimental determination of  $\tau_{\text{rel}}$  can be done via the Fourier transform of the stationary correlation function:

$$C_\varepsilon(\omega) = \int_{-\infty}^{\infty} dt e^{i\omega t} \langle \varepsilon_t \varepsilon_0 \rangle_{\text{stat}} = \frac{Q}{\omega^2 + \tau_{\text{rel}}^{-2}} \quad (4.19)$$

by measuring the line width of this Lorentzian.

<sup>3</sup> The argument here is that the noise sources do not feel the transition because they live on a different time scale

We can use the experimental information that  $\tau_{\text{rel}}$  is of the same order of magnitude for the antisymmetric mode as for the symmetric mode sufficiently far from the transition to check our estimate for the noise strength  $Q$ . Taking  $\tau_{\text{rel}} \approx 0.25$  s and considering the pretransitional range of  $f$  to be 1. to 4. we find  $Q$  ranging from 0.25 to 4. Hz, which is consistent with our previous estimate  $Q=0.25$  Hz (order of magnitude wise). Furthermore we can set out now to determine, on which control curve in the parameter plane ( $a, b$ ) the system approaches the transition. To that end we again assume that  $d \approx 4$  and  $Q \approx 0.25$  Hz do not perceptibly change as the driving frequency is scaled [cf. discussion following (4.17)]. With that we find from

$$4b + a = Qd^2$$

$$4b - a = Qf^2(F)$$

that

$$a(F) = \frac{Qd^2}{2} - \frac{Q}{2} f^2(F), \quad (4.20)$$

$$b(F) = \frac{Qd^2}{8} + \frac{Q}{8} f^2(F), \quad (4.21)$$

where  $f(F)$  is the previously determined function. We have plotted these functions of the driving frequency  $F$  in Fig. 8. Obviously the transition is approached by increasing  $a$ , while  $b$  decreases slightly. We have included the control curve  $b=b(a)$  in the phase portrait of Sect. 2 (Fig. 4).

Independent of these considerations we can determine the set of critical parameters (using again  $d \approx 4$  and  $Q \approx 0.25$  Hz) from the critical condition  $a=4b$ . We find:

$$a_{\text{cr}} = 2.0 \text{ Hz}; \quad b_{\text{cr}} = 0.5 \text{ Hz} \quad (4.22)$$

and we shall use these values to discuss the transients of the transition regime. According to our estimate of  $f$  the last pretransitional parameter plateau corresponds approximately to

$$f_{\text{pre}} = 1.0. \quad (4.22a)$$

We shall use the stationary distribution (4.14) with this parameter value as an initial condition in the next section.

#### 4.4 Transition Region

In the transition region the system, initially prepared in the antisymmetric mode, switches to the symmetric mode, as the antisymmetric mode turns unstable. In the parlance of stochastic theory this means that we expect a transient from an initial distribution centered at  $\phi = \pm \pi$  to a distribution centered at  $\phi = 0$ . To discuss such transient behavior we have to study the

time dependence of the full stochastic system (3.3). We did that by solving the corresponding Fokker-Planck Eq. (3.4) numerically. A one-step integration algorithm for the temporal evolution and a discretization of the interval  $[-\pi, \pi]$  with step size  $\Delta\phi$  were used. The ratio of the time step  $\Delta t$  to  $(\Delta\phi)^2$  was kept at 0.25, which secured stability (cf. e.g. Ames 1977). Periodic boundary conditions were employed. As an initial condition we chose the stationary distribution of the local model of the antisymmetric mode (4.14). The results for the critical parameter values (4.22), determined in the previous section, are depicted in Figs. 9 and 10. Figure 9 illustrates the temporal evolution of  $P(\phi, t)$ . One can clearly see, how the probability mass, initially concentrated at  $\pi$  and  $-\pi$  flows to the central peak at  $\phi=0$ . The resultant distribution is much sharper than the initial one, because  $\phi=0$  is a deeper and steeper minimum of the potential than  $\phi=\pm\pi$  was at the last pretransitional parameter plateau. Figure 10 shows mean and SD evolving in time.  $\langle|\phi_i|\rangle$  quite clearly marks the switching from  $\pm\pi$  to 0. The SD shows how fluctuations are enhanced during the transient (i.e. the distribution is spread out), while they settle to a level even lower than before the transition once the transient has died out. This latter observation again shows that  $\phi_{\text{stat}}=0$  is a more attractive stationary state than  $\phi_{\text{stat}}=\pm\pi$  was before the transition. Let us make the following quantitative observations: (a) We can read off the plots of mean and SD the duration of the transient: this transient time is approximately 2.5–5 s in accord with the experimental estimate of 1–2 s. This result is a true prediction in that the experimental information on  $\tau_{\text{trans}}$  has not been used. A more exact discussion of transient times follows below. (b) The temporal mean of SD is defined as the mean up to the time, when the switching has occurred with 90% probability [i.e. when  $P_\delta(t)$ , defined below in (4.23), first exceeds 0.9]. With that definition we find from the data of Fig. 10: SD = 56 deg. This is the correct order of magnitude as compared to the experimental value of 60 deg (cf. Fig. 3). The corresponding values for the mean phase are 65 deg theoretical and 85 deg experimental. (c) After the transient the SD settles to a stationary value of 6.0 deg, which has to be compared with the experimental 4.5 deg. The corresponding values for the mean phase are 7.3 deg theoretical and 8.0 deg experimental. Again correct orders of magnitudes are obtained.

We performed these same calculations for the parameter setting  $a_{\text{cr}}=1.0$  Hz,  $b_{\text{cr}}=0.25$  Hz, and  $Q=0.125$  Hz, that results, if the larger value for  $\tau_{\text{rel}}=0.5$  Hz is used (cf. Sect. 2). The results are very similar. The switching is somewhat slower (about 5–7 s), but the temporal means and the asymptotic values are identical.

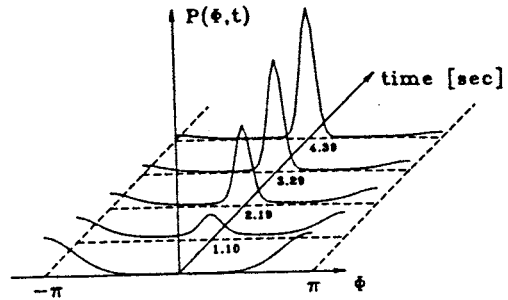


Fig. 9. The temporal evolution of the probability density for the critical parameter values (4.22) is illustrated by showing it at times: 0.0 s, 1.10 s, 2.19 s, 3.29 s, and 4.39 s. All distributions are normalized. The integration parameters were:  $\Delta t = 2.7 \cdot 10^{-3}$  and  $\Delta\phi = 0.11$

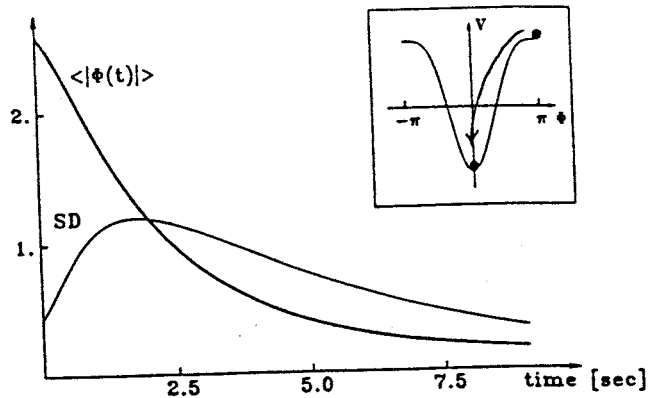


Fig. 10. The mean absolute phase  $\langle|\phi_i|\rangle$  and its SD as a function of time determined from  $P(\phi, t)$  of Fig. 9. The inset shows the potential  $V(\phi)$  at critical parameter values used in Fig. 9 and illustrates the transient motion that occurs during the first 2.5–5 s

A more detailed comparison of theory and experiment would entail time resolved data for the transition regime. Such experiments are under way. Preliminary results show that the transient in SD can be seen (Kelso and Scholz, in preparation). In view of these experimental possibilities we would like to put forward two more exactly defined concepts for the determination of mean transient times in the model. One is the concept of mean first passage time (MFPT), which will be discussed in the subsequent subsection. The other concept makes use of the time dependent solution of the Fokker-Planck equation and can be derived as follows (cf. e.g. Broggi and Lugiato 1984): During the transient, probability mass that is initially concentrated at  $\phi = \pm\pi$  flows to  $\phi=0$  and accumulates there, until the “new” peak at  $\phi=0$  is dominant and stationary. The quantity

$$P_\delta(t) = \int_{-\delta}^{\delta} d\phi P(\phi, t) \quad (4.23)$$

is for adequately chosen  $\delta > 0$  the probability mass of the “new” peak and grows during the transient.



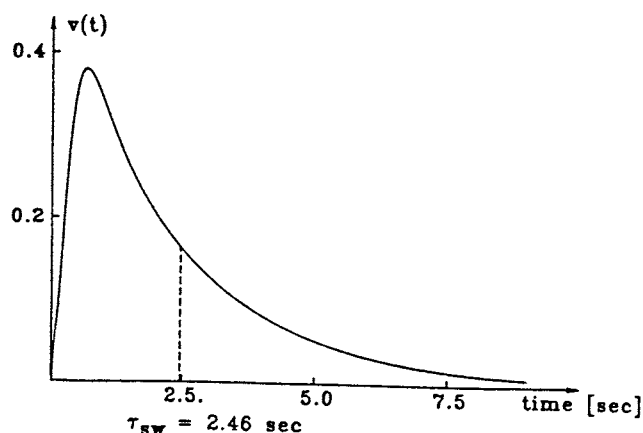


Fig. 11. The switching velocity  $v(t)$  defined by (4.24) as a function of time for the transient at critical parameter values (4.22).  $\tau_{sw}$  is the mean switching time calculated with  $v(t)$  as probability density

$$v(t) = \frac{dP_\delta(t)}{dt} \quad (4.24)$$

is the velocity of this growth, i.e.  $v(t)dt$  is the probability that switching occurs in the time interval  $[t, t+dt]$ . Thus

$$\tau_{switch} = \int_0^\infty tv(t)dt = \int_0^\infty t dP_\delta(t) \quad (4.25)$$

is the mean switching time. This quantity can be compared to an experimentally determined transient time<sup>4</sup>. We have calculated  $v(t)$  for the transient of Fig. 9 [i.e. for the critical parameter values (4.22)]. This is depicted in Fig. 11. The mean switching time from this run is  $\tau_{switch} = 2.5$  s. This is the correct order of magnitude if we compare with the experimental estimate of  $\tau_{trans} = 1$  to 2 s.

Finally we should mention that the transient solutions of the Fokker-Planck equation were also calculated for non-critical parameter values. For pre-transitional parameter setting we found that no switching of the type exhibited in Figs. 9 and 10 occurred. Instead one could observe the equilibration process on a much larger time scale ( $\gg \tau_p = 4$  s) in accord with our time scales argument (4.1). The final state was a comparatively broad distribution with large SD and a mean phase modulus close to  $\pi/2$  (which corresponds to the equidistribution). For posttransitional parameter setting, initial distributions centered at  $\pm\pi$  (which then is an unstable stationary state) relaxed to very sharp distributions centered at  $\phi = 0$  on fast time

<sup>4</sup> A measurement procedure could be as follows: In each of a number of runs one determines the time it takes the system on the transition plateau to first reach a phase with  $|\phi_i| < \delta$  [ $\delta$  of (4.23)]. The arithmetic mean over different runs is then  $\tau_{switch}$

scales of  $\leq 1.0$  s. Thus the transient behavior of Figs. 9 and 10 is indeed characteristic of the critical parameter setting only.

#### 4.5 First Passage Time

The question asked here is: How long does it take before the stochastic relative phase  $\phi_t$  first reaches  $\phi = 0$ , if it was initially at  $\pm\pi$ . This time is a random variable called first passage time and its distribution and moments can be calculated. In the bistable situation below the transition the mean first passage time (MFPT) from  $\pm\pi$  to 0 is a measure of the equilibration time. The reason is that in the equilibration, when an initial distribution evolves towards the stationary distribution, the most arduous and thus slowest process is that of transporting probability mass over a potential hill. But the time scale for this transport is just the MFPT. In our system we expect the MFPT to be large below the transition:  $MFPT \gg \tau_p$ . At the transition the MFPT is a measure of how long it takes before the system first switches to the new stable state  $\phi_{stat} = 0$ . Thus the MFPT is a second theoretical quantity, that can be compared to experimentally determined transition times<sup>5</sup>.

Standard theory gives us a formula for the MFPT that only involves two ordinary integrations (cf. e.g. Gardiner 1983, Sect. 5.2.7b therein). Here we have used the inversion symmetry of the potential to restrict the system to  $[0, \pi]$  only, erecting a reflecting boundary at  $\phi = 0$ .

$$MFPT = \frac{2}{Q} \int_0^\pi dy \psi^{-1}(y) \int_0^y dz \psi(z), \quad (4.26)$$

where

$$\psi(y) = \exp \left[ -\frac{2}{Q} \tilde{V}(y) \right]$$

and

$$\tilde{V}(y) = a \cos y - b \cos 2y.$$

We have evaluated the integrals numerically for various parameter settings. Figure 12 shows the MFPT for  $Q = 0.25$  Hz,  $b = 0.5$  Hz as a function of  $a$  (logarithmic scale). This plot corresponds approximately to the path of the experimental system through the transition (cf. Fig. 8). Note that at  $a = a_{crit} = 2.0$  Hz we have

$$MFPT_{crit} = 4.3 \text{ s} \quad (4.27)$$

again in accord with the experimental estimate of  $\tau_{trans}$ . Obviously the MFPT is very large below the tran-

<sup>5</sup> The mathematical definition of MFPT could be used to devise a different measurement procedure for switching times. We do not want to elaborate this here

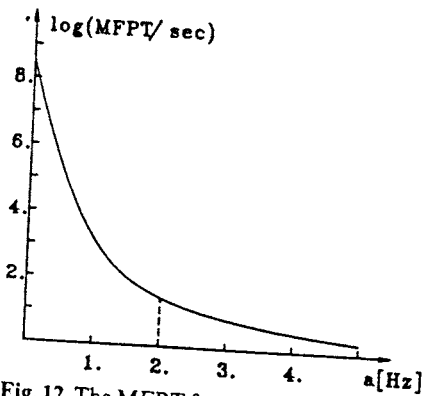


Fig. 12. The MFPT from  $\phi = \pm \pi$  to  $\phi = 0$  plotted logarithmically as a function of  $a$  at  $Q = 0.25$  Hz and  $b = 0.5$  Hz. The value of  $a$  corresponding to the critical parameter set (4.22) is indicated

sition, comes down to the order of  $\tau_p$  only near the transition and drops to values of the order of  $\tau_{rel} \approx 0.25$  s above the transition. Thus for the experimentally relevant parameter values the MFPT is in complete accord with our time scales picture (4.1).

The  $Q$  dependence of the MFPT turned out to be not as sensitive. For example the MFPT varied from 6.4 s to 2.4 s as  $Q$  was varied from 0.1 Hz to 1.0 Hz at  $a = 2$  Hz and  $b = 0.5$  Hz.

## 5 Concluding Remarks

Were one to attempt to count the neurons, neuronal connections, vascular support processes, muscles, and joints that cooperate to produce these "simple" rhythmical motions of the limbs, the result would be a very large number of degrees of freedom. The present paper, however, as well as earlier experimental and theoretical work shows that this high dimensionality can be compressed into a single order parameter that obeys a simple order parameter equation (cf. Haken et al. 1985). The latter is a formal expression of the extremely high degree of coordination among the motor system's many individual components. There is a strong hint that the order parameter used in our work – relative phase – reflects the evolutionary design of rhythmical activity. From the invertebrates, in which many groups use a large number of propulsive structures (e.g., limbs, tube feet, cilia) for swimming and locomotion, to the vertebrates that use one, two, three, or four pairs of legs, the same design feature exists, namely ... "a mechanism for communicating information about the phase of cyclical activity between adjacent members of the system" (Sleigh and Barlow 1980, p. 51). The nature of this phasing information has been recently elaborated (Kelso and Tuller 1985). In addition, phase has been observed to be an essential parameter in many voluntary activities of a less cyclical

kind, ranging from handwriting to speech (e.g., Kelso et al. 1981/1983, for review). It is indicative of a functional constraint on movement or what we call a coordinative structure or unit of action (e.g., Kelso et al. 1979; Kugler et al. 1980; Turvey 1977).

The second major consequence of our studies – treated in detail here – is the decisive role played by fluctuations in initiating a transition between one state and the other at a critical value of the control parameter. This enhancement of fluctuations is exhibited in the numerical solutions of the stochastic model equations and in the experimental data themselves at both kinematic and neuromuscular levels (see Kelso and Scholz 1985). The close agreement between theory and data allows one to interpret the observed changes in modal behavioral patterns as a non-equilibrium phase transition. Further experimental work will evaluate in greater detail certain predictions of the theory, e.g., the various time scale assumptions, explicit calculation of mode relaxation times using Lorentzian functions and perturbation techniques, a fuller characterization of the stochastic nature of fluctuations, etc.

In summary, a serious effort is made here to address the necessary and sufficient conditions for new (or different) forms of spatiotemporal movement patterns to occur. This interplay between coherent motion on the one hand, and instabilities produced by the joint action of scaling influences and fluctuations on the other, is characteristic of pattern formation in many of the multidegree-of-freedom systems treated by synergetics. Thus, it may not be too speculative to suppose that such processes also play a key role in the emergence of the patterned forms of motion produced by animals and people.

*Acknowledgements.* Two of us (H. H. and G. S.) wish to thank the Volkswagenwerk foundation for financial support. J.A.S.K. was supported by ONR Contract N00014-83-C-0083, NIH Grant NS-13617, and BRS Grant RR-05596. We are grateful to John Scholz for comments on an earlier version of the manuscript.

## References

- Ames WF (1977) Numerical methods for partial differential equations. Academic Press, New York
- Broggi G, Lugiatto LA (1984) Transient noise-induced optical bistability. *Phys Rev A* 29:2949
- Gardiner CW (1983) Handbook of stochastic methods for physics, chemistry, and the natural sciences. Springer series in synergetics, vol. 13. Springer, Berlin Heidelberg New York
- Haken H (1975) Cooperative phenomena in systems far from thermal equilibrium and in nonphysical systems. *Rev Mod Phys* 47:67-121
- Haken H (1983) Synergetics: an introduction. Nonequilibrium phase transitions and self-organization in physics, chemistry, and biology. 3rd edn. Springer, Berlin Heidelberg New York

- Haken H, Kelso JAS, Bunz H (1985) A theoretical model of phase transitions in human hand movements. *Biol Cybern* 51:347-356
- Kelso JAS (1981) On the oscillatory basis of movement. *Bull Psychon Soc* 18:63
- Kelso JAS (1984) Phase transitions and critical behavior in human bimanual coordination. *Am J Phys: Reg Integr Comp* 15:R1000-R1004
- Kelso JAS, Scholz J (1985) Cooperative phenomena in biological motion. In: Haken H (ed) *Complex systems-operational approaches in neurobiology, physical systems and computers*. Springer, Berlin Heidelberg New York, pp 124-149
- Kelso JAS, Tuller B (1985) Intrinsic time in speech production: Theory, methodology, and preliminary observations. *Hask Lab Stat Rpt Sp Res SR-81:23-39*. To appear in: Keller E, Gopnik M (eds) *Sensory and motor processes in language*. Erlbaum (in press) Hillsdale, NJ
- Kelso JAS, Southard D, Goodman D (1979) On the nature of human interlimb coordination. *Science* 203:1029-1031
- Kelso JAS, Tuller B, Harris KS (1981) A "dynamic pattern" perspective on the control and coordination of movement. *Hask Lab Stat Rpt Sp Res SR-65:157-196*. Also published in: MacNeilage P (ed) (1983) *The production of speech*. Springer, Berlin Heidelberg New York
- Kugler PN, Kelso JAS, Turvey MT (1980) Coordinative structures as dissipative structures. I. Theoretical lines of convergence. In: Stelmach GE, Requin J (eds) *Tutorials in motor behavior*. North-Holland, Amsterdam
- Schmidt RA (1982) Motor control and learning: a behavioral emphasis. Champaign, IL, Human Kinetics
- Sleigh MA, Barlow DI (1980) Metachronism and control of locomotion in animals with many propulsive structures. In: Elder HY, Trueman ET (eds) *Aspects of animal locomotion*. Cambridge University Press, Cambridge
- Turvey MT (1977) Preliminaries to a theory of action with reference to vision. In: Shaw R, Bransford J (eds) *Perceiving, acting and knowing: toward an ecological psychology*. Erlbaum Hillsdale, NJ

Received: September 27, 1985

Prof. Dr. Dr. h.c. H. Haken  
 I. Institut für theoretische Physik  
 Universität Stuttgart  
 Pfaffenwaldring 57/4  
 D-7000 Stuttgart 80  
 Federal Republic of Germany